

Nonlinear dynamics for estimating the tip radius in atomic force microscopy

Rull Trinidad, E.; Gribnau, T.W.; Belardinelli, P.; Staufer, U.; Alijani, F.

DOI

[10.1063/1.4991471](https://doi.org/10.1063/1.4991471)

Publication date

2017

Document Version

Final published version

Published in

Applied Physics Letters

Citation (APA)

Rull Trinidad, E., Gribnau, T. W., Belardinelli, P., Staufer, U., & Alijani, F. (2017). Nonlinear dynamics for estimating the tip radius in atomic force microscopy. *Applied Physics Letters*, 111(12), Article 123105. <https://doi.org/10.1063/1.4991471>

Important note

To cite this publication, please use the final published version (if applicable). Please check the document version above.

Copyright

Other than for strictly personal use, it is not permitted to download, forward or distribute the text or part of it, without the consent of the author(s) and/or copyright holder(s), unless the work is under an open content license such as Creative Commons.

Takedown policy

Please contact us and provide details if you believe this document breaches copyrights. We will remove access to the work immediately and investigate your claim.

Nonlinear dynamics for estimating the tip radius in atomic force microscopy

E. Rull Trinidad, T. W. Gribnau, P. Belardinelli, U. Staufer, and F. Alijani^{a)}

Department of Precision and Microsystems Engineering, TU Delft, Mekelweg 2, 2628CD Delft, The Netherlands

(Received 21 June 2017; accepted 9 September 2017; published online 21 September 2017)

The accuracy of measurements in Amplitude Modulation Atomic Force Microscopy (AFM) is directly related to the geometry of the tip. The AFM tip is characterized by its radius of curvature, which could suffer from alterations due to repetitive mechanical contact with the surface. An estimation of the tip change would allow the user to assess the quality during imaging. In this work, we introduce a method for tip radius evaluation based on the nonlinear dynamic response of the AFM cantilever. A nonlinear fitting procedure is used to match several curves with softening nonlinearity in the noncontact regime. By performing measurements in this regime, we are able to maximize the influence of the tip radius on the AFM probe response, and this can be exploited to estimate with good accuracy the AFM tip radius. *Published by AIP Publishing.*

[<http://dx.doi.org/10.1063/1.4991471>]

Atomic Force Microscopy (AFM) has evolved into one of the most powerful tools in nanotechnology.^{1–3} Through the introduction of different operating modes, AFM is increasingly being used in metrology for industrial applications.⁴ The force interaction between the AFM tip and the sample is used to measure topography or other nanomechanical properties such as roughness or hardness. In the Amplitude Modulation mode (AM-AFM), surfaces are scanned with a resonating microcantilever that is driven at or near its first resonance frequency, and with every oscillation, the tip briefly touches the sample. A feedback loop keeps the vibration amplitude constant by adapting the distance between the sample and the base of the cantilever.

The resolution that can be achieved with AM-AFM is highly dependent on the tip sharpness. Difficulties in obtaining a precise tip radius calibration method have been pointed out in the literature.⁵ In order to provide commercially viable processes with high quality measurements, it is desired to continuously assess the tip condition in between or even during measurements. By using a Scanning Electron Microscope (SEM), high-precision images with nanometer resolution can be obtained. However, the full reliability of the method is affected by the uncertainty on the angle at which the two-dimensional image is captured. The contamination of the AFM tip is another important limiting factor of this approach. A more realistic 3D tip-shape characterization methodology is the “Blind Tip Reconstruction.”⁶ This technique has an increased risk of tip damage due to the additional tip-approach and scanning of the topographically challenging surface. Therefore, an accurate and safe *in-situ* estimation of the AFM tip radius is still an open research question. Using static mode force-spectroscopy, the nonlinear van der Waals forces have been analysed for fitting the values of the tip radius by data obtained from force-distance curves in the attractive regime.^{7,8} Dynamic mode AFM could potentially be another nondestructive way of estimating the tip radius during AFM measurements. In this mode, the

information is obtained directly from the vibrations of the cantilever, which is essentially a repetitive approach curve. The analysis of the probe-surface interaction can be done by the acquisition of vibration amplitude vs. distance curves, the use of amplitude-frequency response curves, or by extracting the Fourier spectrum of the driving signal.⁹ Exploring the first option, Santos *et al.* developed a method that is mostly empirical to identify the tip sharpness by obtaining approach/retract curves and inspecting the transitions from attractive to repulsive force regimes.¹⁰ A study carried out by Holscher *et al.*¹¹ shows that the tip-sample potential can be experimentally obtained by measuring the shift of the resonance frequency as a function of the resonance amplitude of the AFM cantilever in frequency modulation. Hu *et al.* showed that the nonlinear behaviour of AFM cantilevers interacting with a sample can be exploited for parametric studies estimating the Hamaker constant by means of a harmonic balance based identification method.¹²

In this letter, we report a parametric study of the frequency response of the oscillating cantilever in the noncontact mode and its use for assessing the tip radius. In this operating mode, the cantilever is periodically excited with a dither piezo at a distance of a few nanometers above the sample surface. The nonlinear response of the cantilever is then directly related to the van der Waals interaction potential between the sample surface and the AFM tip, which is proportional to the tip radius. Our theoretical study consists of a lumped parameter model subjected to the harmonic excitation and van der Waals tip-sample interaction.¹³ The simulations in the attractive regime have been validated by experiments, and the nonlinearity of the tip-sample interaction has been demonstrated by experimental curves representing the amplitude-frequency relationship. A schematic representation of the situation is illustrated in Fig. 1.

The tip of the AFM probe in its rest position has a distance z_c from the sample. The amplitude of the oscillation around this reference position is indicated by the variable z . The interaction between the probe and the surface in the attractive regime is given by

^{a)}Electronic mail: f.aliyani@tudelft.nl

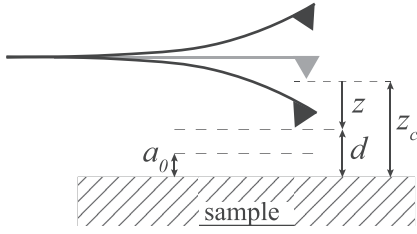


FIG. 1. Schematic of the AFM and the sample. The rest position of the cantilever is the reference for the deflection z .

$$F_{\text{int-vdW}}(z) = -\frac{HR^{(1+\alpha)}}{6(z_c + z)^{(2+\alpha)}}, \quad d \geq a_0 \quad (1)$$

in which α assumes a value 0 or 1 in the case of a (hemi-)spherical or a flat circular tip,¹⁴ respectively. H represents the Hamaker constant, R the tip radius, and a_0 the intermolecular distance, respectively. When the tip-sample distance $d = z_c + z$ is smaller than a_0 , other models apply for the AFM cantilever oscillation such as the Derjaguin-Muller-Toporov (DMT).¹⁵ The DMT model combines an attractive van der Waals model governing the noncontact behaviour ($d \geq a_0$) and a Hertzian contact formulation ($d < a_0$), which is proportional to the square root of R . However, the tip sample force expressed in Eq. (1) is either linearly dependent on R ($\alpha = 0$) or quadratically dependent ($\alpha = 1$), in the purely attractive domain. Thus, the conformation of the dynamical response as a function of the tip radius can be more easily determined by exploiting the noncontact region.

In AFM experiments, a lock-in amplifier is used to measure the amplitude and phase of the cantilever deflection signal with no contribution from higher modes and the absence of any internal resonance.¹⁶ It is therefore valid to model the cantilever as a single-degree-of-freedom model as follows:

$$m \frac{d^2 z}{dt^2} + \frac{m\omega_n}{Q} \frac{dz}{dt} + k_c z = F \cos(\omega t) - \frac{HR^{(1+\alpha)}}{6(z_c + z)^{(2+\alpha)}}. \quad (2)$$

The cantilever beam with effective mass m and spring constant k_c is actuated by a sinusoidal external signal with amplitude F and angular frequency ω ; Q and ω_n are the quality factor and the angular resonance frequency, respectively.

To perform a parametric study, the nondimensional form of Eq. (2) is considered

$$\frac{d^2 \hat{z}}{d\tau^2} + \hat{c} \frac{d\hat{z}}{d\tau} + \hat{z} = \lambda \cos(\hat{\Omega}\tau) - \beta \frac{1}{(1 + \hat{z})^{(2+\alpha)}}, \quad (3)$$

in which the dimensionless deflection and dissipation coefficient are $\hat{z} = \frac{z}{z_c}$ and $\hat{c} = \frac{1}{Q}$, respectively. The dimensionless time is $\tau = \omega_n t$, whereas $\lambda = \frac{F}{z_c k_c}$ represents the coefficient of the sinusoidal excitation with frequency $\hat{\Omega} = \frac{\omega}{\omega_n}$. The nonlinear interaction is governed by the coefficient $\beta = \frac{HR^{(1+\alpha)}}{6k_c z_c^{(3+\alpha)}}$. Assuming R as a sole varying parameter in Eq. (2), the frequency response of the system as a function of the tip-radius is reported in Fig. 2. The presented frequency response curves were calculated with a pseudo-arc length continuation and bifurcation software package,¹⁷ which allows us to follow the solution path and obtain stable and unstable solutions. The

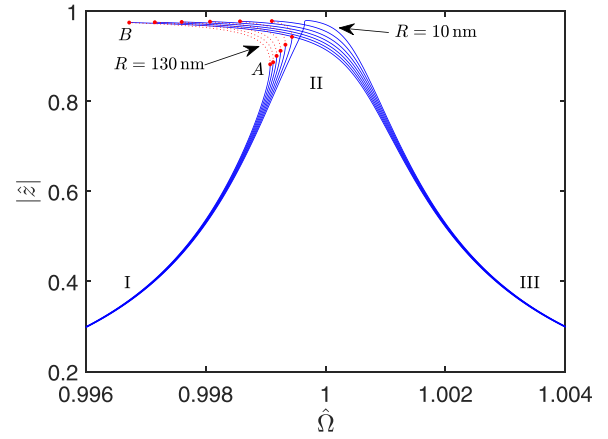


FIG. 2. Frequency response for different values of R for a (hemi-)spherical tip (from left to right, $R = \{130, 110, 90, 70, 50, 30, \text{ and } 10\}$ nm). For the numerical simulation, we considered $z_c = 20$ nm and $H_{\text{Si-HOPG}} = 2.9656 \times 10^{-20}$ J. In the normalized amplitude, a value in the ordinate equal to 1 indicates the position of the sample surface ($z = -z_c$). Regions I–III are used for the fitting procedure.

simulation analysis begins at the zero force level where the initial solution corresponds to the undeformed configuration of the system by choosing the excitation amplitude (λ) as the continuation parameter at a fixed excitation frequency far from resonance (e.g., $\omega < \omega_n$). Once the desired force level is reached, the solution continues by considering the dimensionless excitation frequency ($\hat{\Omega}$) as the continuation parameter to obtain the frequency-amplitude response of the cantilever.

The frequency response in the attractive regime is governed by a softening behaviour as shown in Fig. 2. The large values of the tip radius affect the position of the saddle-node points (points A and B, respectively), moving the peak of the response towards lower frequencies. Here, we remark that the implemented model analyses the motion only for the configuration for which $d \geq a_0$.

This theoretical behaviour has also been experimentally investigated. A commercial AFM (Nanosurf FLEX operated with the C3000 controller) was used to statically approach the inspected AFM cantilever towards the sample and to keep the reference distance z_c of the tip with respect to the surface constant during the remainder of the experiment. An external multi-frequency lock-in analyzer (Intermodulation Products AB), directly connected to the AFM unit, excited the cantilever to allow the dynamic analysis. The cantilever probes used in the experiments are commercially available (NCLR, NanoWorld AG) with a nominal tip radius of 8 nm as indicated by the supplier. The sample used was Highly Oriented Pyrolytic Graphite (HOPG). For each experiment, a calibration of the spring constant k_c of the cantilever based on a noninvasive method was performed¹⁸ and the relative humidity was controlled ($< 10\%$).

In order to obtain the experimental frequency response curves with a repeatable and systematic method, the following steps were defined: (i) the cantilever was approached to the sample in the static mode (approach phase); (ii) a force-distance curve was acquired recording the effective deflection of the cantilever. The forward motion was stopped at a small, arbitrarily chosen, cantilever deflection set point of 2 nm. The corresponding position was considered to be at the

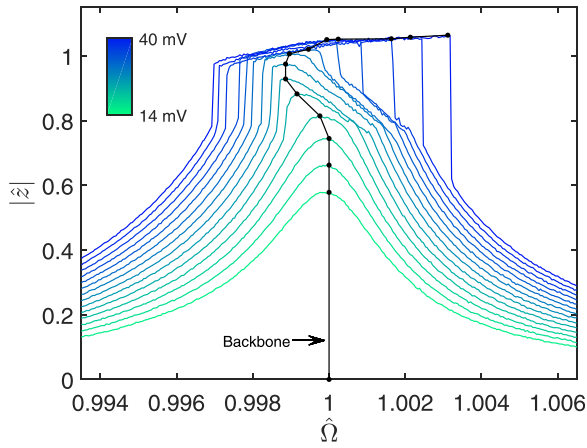


FIG. 3. Experimental frequency response curves with increasing excitation amplitude. The color code indicates an increase in excitation (2 mV steps were made). The solid line indicates the backbone curve, and the sample is at $z_c = 20$ nm.

surface, i.e., where $d \approx a_0$; (iii) the cantilever was pulled back from the sample with a fixed backward length (the backward length corresponds to the distance from sample z_c); (iv) a closed-loop-controller on the z -axis motion was activated to avoid drifting away from this position; (v) the frequency was swept in the specified neighbourhood of the estimated resonance frequency and the vibrational amplitude was measured in order to obtain the experimental curves.

To investigate the tip-radius effect by minimizing the dangerous and most often destructive repulsive interaction with the sample, it is important to identify the noncontact regime.^{19,20} This can be done by sweeping the excitation frequency from below the resonance frequency to above and back again. Instead of reducing z_c in the free-air amplitude while keeping the excitation F constant, also F can be increased while z_c is being kept constant. The experimental results of the dynamical response with respect to the

increasing values of the excitation amplitude are reported in Fig. 3.

The accuracy with which the responses were measured permitted to clearly identify the transition from the purely attractive to the repulsive region. It can be seen from the so-called “backbone curve” (black line in Fig. 3) that the response was first governed by the softening behaviour due to the van der Waals forces, whereas it transitioned into hardening when the amplitude of the tip surmounted the intermolecular distance a_0 . With the information collected by the backbone curve, it was possible to verify that the chosen distance (z_c) and the excitation force amplitude were in the noncontact regime.

For the identification process, the properties of the cantilever and the Hamaker constant were assumed to be known. The height of the frequency response curves (regions I and III in Fig. 2) was primarily determined by F and the width (region II) by Q . Next, the positions of the saddle-node points (points A and B in Fig. 2) connecting the stable and unstable motion were matched considering the tip radius R as the fit parameter. Due to the softening nature of the curves, obtaining the data from the backward sweep was crucial for the fitting. An estimated uncertainty in a z_c value of ± 1 nm was taken into account for the fitting procedure and a Hamaker constant $H_{\text{Si-HOPG}} = 2.9656 \times 10^{-20}$ J.¹² In Fig. 4, we report for three different cantilevers the experimental frequency response curves and their corresponding fit interacting with the HOPG sample. To finish the experiments, the tip was removed without any additional approaching of the probe towards the sample and inspected using a SEM.

The experimental curves shown in Fig. 4(a) are fitted with a spherical tip radius of $R = 19 \pm 6$ nm. The obtained value of the tip radius is in good agreement with the extracted value from the SEM image that gives $R = 18 \pm 2.7$ nm. The tip radius estimation in Fig. 4(b) was obtained, accounting for a blunted tip interaction ($R = 12 \pm 1.5$ nm), and is in good

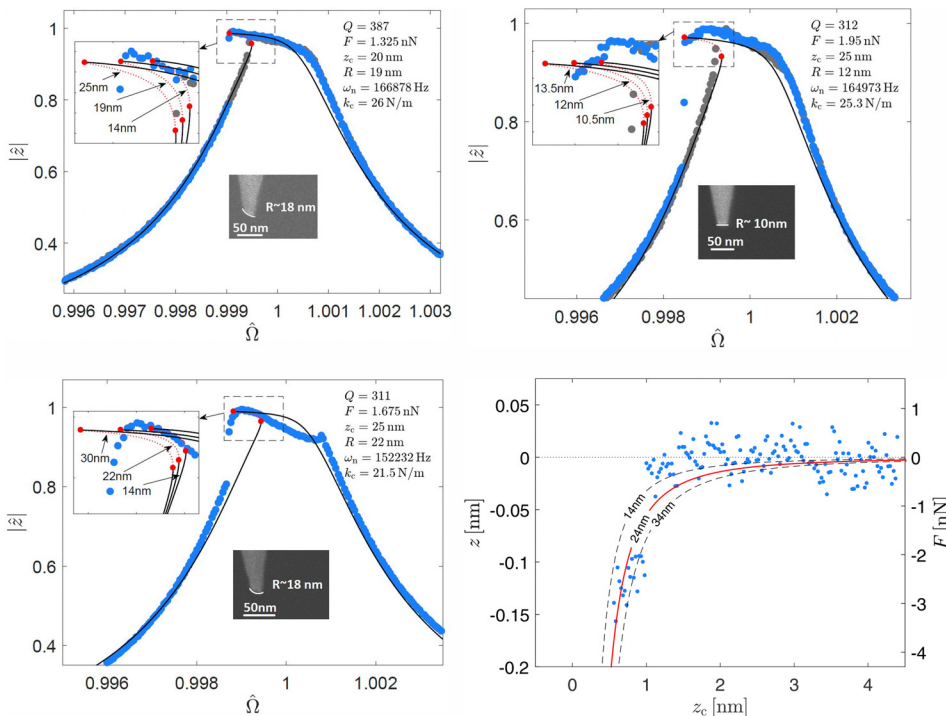


FIG. 4. Experiments using different cantilevers. For figures (a)–(c), the theoretical model is depicted with a black line and the experimental data are represented by grey dots (frequency sweep forward) and blue dots (frequency sweep backward). The inset SEM image of the AFM tip is shown for all cases. (d) The tip radius static deflection fit corresponding to the van der Waals force in the approach phase of the cantilever in (c).

agreement with the SEM measurement for a flat circular tip ($R = 10 \pm 2$ nm). It should be noted that, by applying to this set of experiments the (hemi-)spherical model, the order of magnitude of the estimated value remains preserved ($R = 60 \pm 18$ nm), although there is a large discrepancy between the SEM and the identified tip radius. This underlines that the (hemi-)spherical model could be a precautionary model if an *in-situ* tip estimation is to be performed since it provides a safer threshold for avoiding undesired tip deterioration. In Fig. 4(c), a similar experiment was performed on a third cantilever by finding the frequency response curve only in the backward sweep. In this case, the tip radius ($R = 22 \pm 8$ nm) is also close to the value by the SEM image ($R = 18 \pm 4$ nm). However, to have a better comparison, the force-distance spectroscopy measurement for the third cantilever is also obtained and presented in Fig. 4(d). As it can be observed, a static fit accounting for the interactions described in Eq. (1) could be achieved for a range with an optimal $R = 24 \pm 10$ nm, which is within the tolerances of the estimation obtained by the current dynamic method. It is worth noting that, compared to the performed force-distance measurement, our method assesses the tip condition by looking solely at the frequency response curves in the attractive regime and thus does not allow further contact with the sample during tip assessment.

In summary, a methodology to determine the AFM tip radius has been presented. The method consists of the acquisition of frequency response curves in the attractive regime where the influence of the tip radius is predominant. The experimental frequency response curves are fitted to the model that includes the van der Waals force. It is found that exploiting the nonlinear dynamic response of the cantilever is a safe method for tip assessment.

This work was performed within the aim4np project, which was supported by the EC through a grant (Contract No. 309558) within the 7th Frame-work Program.

- ¹G. Binnig, C. F. Quate, and C. Gerber, *Phys. Rev. Lett.* **56**, 930 (1986).
- ²Y. Martin, C. C. Williams, and H. K. Wickramasinghe, *J. Appl. Phys.* **61**, 4723 (1987).
- ³F. J. Giessibl, *Rev. Mod. Phys.* **75**, 949 (2003).
- ⁴G. Schitter, J. Steininger, F. C. Heuck, and U. Staufer, *Int. J. Nanomanuf.* **8**, 392 (2012).
- ⁵R. W. Stark, *Mater. Today* **13**, 24 (2010).
- ⁶J. S. Villarrubia, *J. Res. Nat. Inst. Stand. Technol.* **102**, 425 (1997).
- ⁷C. Argento and R. H. French, *J. Appl. Phys.* **80**, 6081 (1996).
- ⁸I. Siretanu, D. Ebeling, M. P. Andersson, S. L. S. Stipp, A. Philipse, M. C. Stuart, D. van den Ende, and F. Mugele, *Sci. Rep.* **4**, 4956 (2014).
- ⁹F. Gramazio, M. Lorenzoni, F. Pérez-Murano, E. Rull Trinidad, U. Staufer, and J. Fraxedas, *Beilstein J. Nanotechnol.* **8**, 883 (2017).
- ¹⁰S. Santos, L. Guang, T. Souier, K. Gadelrab, M. Chiesa, and N. H. Thomson, *Rev. Sci. Instrum.* **83**, 043707 (2012).
- ¹¹H. Hölscher, W. Allers, U. D. Schwarz, A. Schwarz, and R. Wiesendanger, *Phys. Rev. Lett.* **83**, 4780 (1999).
- ¹²S. Hu, S. Howell, A. Raman, R. Reifenberger, and M. Franchek, *J. Vib. Acoust.* **126**, 343 (2004).
- ¹³R. García and A. San Paulo, *Phys. Rev. B* **60**, 4961 (1999).
- ¹⁴D. Ebeling, D. van den Ende, and F. Mugele, *Nanotechnol.* **22**, 305706 (2011).
- ¹⁵B. Derjaguin, V. Muller, and Y. Toporov, *J. Colloid Interface Sci.* **53**, 314 (1975).
- ¹⁶P. N. Kambali, G. Swain, A. K. Pandey, E. Buks, and O. Gottlieb, *Appl. Phys. Lett.* **107**, 063104 (2015).
- ¹⁷E. J. Doedel, A. R. Champneys, F. Dercole, T. F. Fairgrieve, Y. Kuznetsov, B. E. Oldeman, R. C. Paffenroth, B. Sandstede, X. J. Wang, and C. H. Zhang, AUTO-07p: Continuation and bifurcation software for ordinary differential equations, Department of Computer Science, Concordia University, Montreal, Canada, 2010; available at <http://cmvl.cs.concordia.ca/auto/>.
- ¹⁸M. J. Higgins, R. Proksch, J. E. Sader, M. Polcik, S. M. Endoo, J. P. Cleveland, and S. P. Jarvis, *Rev. Sci. Instrum.* **77**, 013701 (2006).
- ¹⁹S. Crittenden, A. Raman, and R. Reifenberger, *Phys. Rev. B* **72**, 235422 (2005).
- ²⁰A. Kuhle, A. H. Sorensen, and J. Bohr, *J. Appl. Phys.* **81**, 6562 (1997).